Journal of
Hazardous Materials

Numerical simulation of turbulent gas flames in tubes

E. Salzano [a,*], F.S. Marra [a], G. Russo [b], J.H.S. Lee [c]

[a] *Istituto di Ricerche sulla Combustione, CNR-IRC, Napoli, Italy*
[b] *Dipartimento di Ingegneria Chimica, Università di Napoli "Federico II", Napoli, Italy*
[c] *Department of Mechanical Engineering, McGill University, Montreal, Que., Canada*

Abstract

Computational fluid dynamics (CFD) is an emerging technique to predict possible consequences of gas explosion and it is often considered a powerful and accurate tool to obtain detailed results. However, systematic analyses of the reliability of this approach to real-scale industrial configurations are still needed. Furthermore, few experimental data are available for comparison and validation.

In this work, a set of well documented experimental data related to the flame acceleration obtained within obstacle-filled tubes filled with flammable gas–air mixtures, has been simulated. In these experiments, terminal steady flame speeds corresponding to different propagation regimes were observed, thus, allowing a clear and prompt characterisation of the numerical results with respect to numerical parameters, as grid definition, geometrical parameters, as blockage ratio and to mixture parameters, as mixture reactivity.

The CFD code AutoReagas© was used for the simulations. Numerical predictions were compared with available experimental data and some insights into the code accuracy were determined. Computational results are satisfactory for the relatively slower turbulent deflagration regimes and became fair when choking regime is observed, whereas transition to quasi-detonation or Chapman–Jogouet (CJ) were never predicted.
© 2002 Elsevier Science B.V. All rights reserved.

Keywords: Gas explosion; CFD simulation; Premixed flames; Flame acceleration; Turbulent flame

1. Introduction

The study of flame acceleration in the presence of obstacles is important as far as safety within industrial environments is concerned. A high level of confinement due to obstacle

---

* Corresponding author. Tel.: +39-8176-21922; fax: +39-8176-22915.
E-mail address: salzano@irc.na.cnr.it (E. Salzano).

Nomenclature

a	orifice section (m^2)
A	tube section (m^2)
BR	blockage ratio ($1 - d^2/D^2$)
C_D	drag coefficient
C_t	dimensionless turbulent constant in Eq. (1)
C_μ	constant of k–ε model
C_1	constant of k–ε model
C_2	constant of k–ε model
d	orifice diameter (m)
D	tube diameter (m)
F_k	fraction of turbulent kinetic energy loss by drag
F_s	stretching factor in Eq. (3)
k	turbulent kinetic energy ($m^2\,s^2$)
L	length of tube (m)
L_t	turbulent length scale (m)
r	radius of spherical flame (m)
R_c	reaction rate ($kg\,m^{-3}\,s^{-1}$)
R_{min}	minimum mass fraction
S_f	flame speed ($m\,s^{-1}$)
S_l	laminar burning velocity ($m\,s^{-1}$)
$S_{l,eff}$	effective laminar burning velocity ($m\,s^{-1}$)
S_t	turbulent burning velocity ($m\,s^{-1}$)
u_t	turbulent intensity ($m\,s^{-1}$)
u_i	velocity ($m\,s^{-1}$)

Greek letters

ε	dissipation of turbulent kinetic energy ($m^2\,s^3$)
ϕ	equivalence ratio
Γ	turbulent diffusion coefficient ($m^2\,s^{-1}$)
ν	kinematic viscosity ($m^2\,s^{-1}$)
ρ	density ($g\,m^3$)
σ_ε	constant of k–ε model
σ_k	constant of k–ε model

congestion often characterises chemical plants handling flammable gases. The interaction of the flame with the obstacles promotes strong mixing and hence turbulent combustion in the flame zones.

A possible approach to the analysis of such phenomena in real large scale scenario is represented by the use of computational fluid dynamics (CFD) based codes, which allows a detailed description of the explosion behaviour once appropriate sub-models for turbulence and combustion are specified [1–3]. These codes have been "validated" against experiments

of up to full-scale geometry. However, due to the complexity of the involved phenomena, they are often "calibrated" against experimental data (usually the overpressure) and may not provide independent means of assessing their ability in describing the turbulent flame acceleration mechanism. It is worth noting that the disparity between length scales—ranging from small obstacles to the size of the entire plant—and time scales (e.g. laminar to turbulent combustion rate) prohibits the use of direct simulation of turbulence and combustion as far as real configuration is concerned, due to the unaffordable amount of computational power and time.

Aim of this work is to provide an illustrative example of comparison between an available set of experimental data and the corresponding numerical simulation results obtained adopting simple models and coarse grids, as often required for the computation of real configuration. Out the scope of this work is the intent to obtain the best result for a single test case. Indeed, several papers have been dedicated to this last objective by the numerical simulation community, but little attention have been devoted to assessing the reliability of a single code varying the physical scenario.

It is well established that rapid flame acceleration can be achieved in tubes filled by obstacles [4–7]. Flame speeds ranging from tens to hundreds of meters per second are reached, depending on the fuel type, mixture composition and boundary condition, i.e. tube geometry and obstacles configuration. When highly reactive gases like hydrogen and acetylene are considered, transition to the "quasi-detonation" and normal Chapman–Jogouet (CJ) detonation regimes are also observed.

The main mechanism for the flame acceleration is represented by the turbulence generated in the unburned mixture ahead of the flame front. Indeed, the obstacles provide a powerful source of "randomisation" of the mean flow kinetic energy. Moreover, the interaction of the flame with the obstacles also promotes strong mixing in the flame zone.

The transient turbulent flame acceleration process is very complex and large local fluctuations are even found in the laboratory experiments. However, some universal trends have been reported for very long tubes filled by obstacles and "steady state" regimes have been recognised. The "quenching regime" is the slowest among these regimes and it only appears when very high blockage ratios are considered. This regime is of very little interest in safety application. Next, the "weak turbulent flame regime" develops with fuel–air mixtures characterised by low reactivity. Typical flame speeds for this regime are of the order of $<100\,\mathrm{m\,s^{-1}}$. The "choking regime" is governed by the reactivity of the mixture: the flame speeds correspond closely to the sound speed of the combustion products (i.e. about $800\,\mathrm{m\,s^{-1}}$ for most hydrocarbons). Flame speeds of about $1200\,\mathrm{m\,s^{-1}}$ are observed in the case of transition of flame propagation to the "quasi-detonation regime". Finally, flame speeds of about $2500\,\mathrm{m\,s^{-1}}$ are observed when the "Chapman–Jouguet detonation regime" is reached.

In the present study, the CFD code AutoReagas© developed by TNO (NL) and Century Dynamics (UK) and available by the CNR-GNDRCIE (National Research Council) in Naples, Italy, was used to predict the flame speed observed in tubes filled by obstacle and different flammable mixtures. The capability of the code in reproducing the maps of propagation velocities developed by the experimental work carried out at the McGill University have been determined. Estimates of the validity limits of numerical results have been performed.

2. The CFD code AutoReagas©

AutoReagas© solves the conservation equations for mass, energy and momentum by the finite volume formulation [8]. The turbulent flow field is described by the k–ε model [9]. Combustion reaction is considered as a single-step conversion from reactants to products and the volume based combustion rate, R_c, to be included in the mass conservation equation, is computed as

$$R_c = C_t \rho \frac{S_t^2}{\Gamma} R_{\min} \tag{1}$$

where ρ is the mixture density, Γ the turbulent diffusion coefficient for mass and/or energy, $R_{\min}$ the minimum mass fraction among those of fuel, oxygen and products and C_t is a dimensionless constant, which represents the main adjustable parameter and was set on the base of previous sensitivity analyses [2,10]. The turbulent burning velocity S_t is expressed through the Bray correlation [11]:

$$S_t = 1.8 u_t^{0.412} L_t^{0.196} S_l^{0.784} \nu^{-0.196} \tag{2}$$

where u_t is the turbulence intensity, L_t the turbulent macroscale, S_l the laminar burning velocity, and ν is the kinematic viscosity of the unburned mixture. Further details about the code are reported in [12].

According to Eqs. (1) and (2), the only physical mechanism of flame acceleration implemented in AutoReagas© is the burning rate enhancement due to the flow turbulence generated ahead of the flame front. This mechanism dominates the obstacle-filled tube explosions. Hence, the experimental data obtained with such configurations are particularly suitable for validating the AutoReagas© code.

A quasi-laminar modification [13] is used for the initial laminar combustion rate. The effects of pressure, temperature and flame front wrinkling on the laminar burning velocity are described by a second adjustable parameter F_s which relates $S_{l,eff}$ to the flame radius r and to the theoretical laminar flame speed:

$$S_{l,eff} = S_l(1 + F_s r) \tag{3}$$

The full set of constants used for the simulation is reported in Table 1.

Table 1
The set of constants used for the CFD simulations [6,8–13]

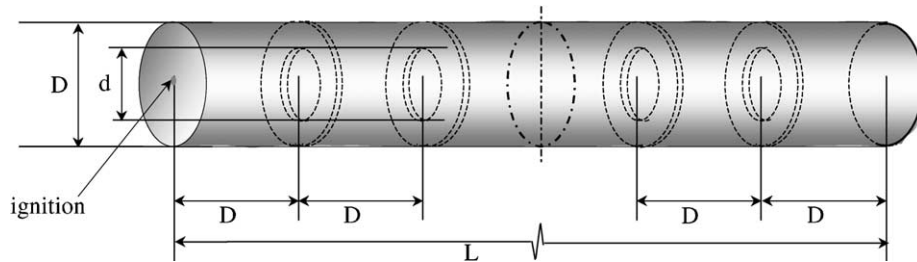| Constant	Value
Combustion rate	
Laminar F_s (Eq. (3))	0.25
Turbulent C_t (Eq. (1))	100
k–ε model	
C_μ	0.09
C_1	1.44
C_2	1.79
σ_k	1.0
σ_ε	1.3
F_k	0.5

Fig. 1. Geometry of the closed tubes filled by circular orifice rings (case (a)).

3. Results and discussion

3.1. Experimental set-up

The experimental configurations reproduced in the numerical simulations are sketched in Figs. 1 and 2.

Case (*a*) (*circular tubes*): Steel tubes 11 and 18 m long (*L*), diameters (*D*) of 0.05, 0.15 and 0.3 m have been considered [4,6]. The tubes are closed at both ends and ignition is provided at one end of the tube by an electric spark. Circular orifice rings spaced one diameter *D* apart are installed. Three different blockage ratios (BR $= 1 - d^2/D^2$, where *d* is the orifice diameter) of 0.44, 0.39 and 0.28 are adopted. This configuration well represents the case of turbulence mixing introduced at a scale comparable to the diameter of the tube.

The AutoReagas$^©$ code allows only a Cartesian co-ordinate system. Therefore an equivalent diameter has been used to transform the circular section to the square section.

Case (*b*) (*rectangular tubes*): Vertical circular rods with 0.034 m diameter fill a steel tube with a square cross-section of 0.3 m side, 7 m long [14]. The cylinders are arranged in 3×2 pattern spaced one tube width apart (0.3 m). The average blockage ratio of the 3×2 obstacle array is 0.41. The tube is closed at both ends and ignition is provided at one end of the tube
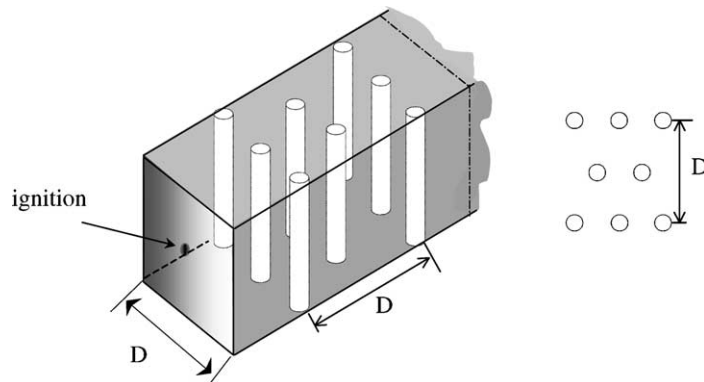

Fig. 2. Square tube filled by circular rods (case (b)).

by an electric spark. In this case turbulence mixing is introduced at a smaller scale and in a more effective way.

As it will be described later, despite the disparity in both shape and dimensions of objects, the level of description attained by the adoption of very coarse grids results very similar for the cases (a) and (b): the only difference is the value of the effective "sub-grid" turbulence generation term.

3.2. Numerical results

The numerical flame speed along the tube has been obtained by means of the computed combustion rate histories. Specifically, the time of arrival of the flame at a specific location has been assumed to correspond to the time when the maximum combustion rate is attained.

We assume that the flame speed shows an asymptotic trend to the terminal flame speed for all tests. This assumption is well supported by experimental evidence in tubes characterised by a large value of the scale parameter L/D. Then, the terminal steady flame speed is computed averaging the flame position over the time for the last 3 m of the tube.

3.2.1. Effect of object definition

AutoReagas$^{©}$ allows two different models to account for the presence of the obstacles. They can be either defined as "solids objects", i.e. as solid boundaries within the computational domain, or as "sub-grid", i.e. as additional turbulence sources within the specified computational cells. In the latter case, appropriate values of the drag coefficient (C_D) and turbulent length scale (L_t) must be assigned for any cell containing sub-grid object and a source term is then added in the turbulent kinetic energy equation, having the form

$$S_{KS} = F_k C_D \frac{1}{2} \rho |u_i|^3 \tag{4}$$

where u_i is the velocity and F_k is an additional universal model constant included to take into account the fraction of turbulent kinetic energy loss by drag (see [2] for more details on the sub-grid models).

To investigate the effect of the two different way of modelling, a numerical grid of about 250,000 cubic cells (2500 × 10 × 10 cells along x-, y-, and z-axis), side 5 mm, has been considered in order to reproduce the experimental data obtained for the case (a), tube diameter 0.05 m, 11 m long, BR = 0.44, filled by stoichiometric methane–air mixture. The orifice rings were defined either solid or sub-grid. The "solid" option can only be used if the object dimension is larger than the cell size, otherwise being the sub-grid option mandatory. However, code developers highly recommend the sub-grid option, unless the objects are much larger than cell size. In the case of sub-grid modelling, C_D and the turbulent length scale L_t has been set to 2 and 20% of the obstacle cross-flow dimension, respectively [2,15].

The predicted terminal steady flame speeds are $835 \, \text{m s}^{-1}$ adopting the sub-grid option and $750 \, \text{m s}^{-1}$ adopting the solid option. A difference of about 4 and 6% with respect to the experimental value of $800 \, \text{m s}^{-1}$ is then observed. The terminal steady flame speed obtained using the solid option shows that the predicted turbulence intensities are too low to reproduce the experimental value. It is worth to note that the turbulent flow field induced by small-scale obstacles is not adequately computed if the solid option is adopted, because of the "slip" condition imposed at the object wall. On the other hand, the adoption of the sub-grid
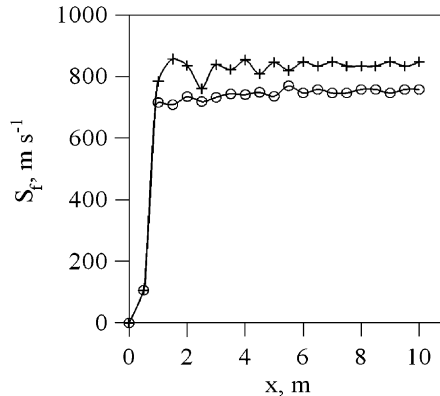
Fig. 3. Flame speed computed along the tube axis for the case (a): BR $= 0.44$, $L = 11\,\text{m}$, $\phi = 1$; (+) sub-grid option; (○) solid option.

modelling introduces three new empirical constants (C_D, L_t, and F_k) in order to control the turbulence intensity. It appears that the suggested values are adequate to reproduce the right flame speed within a good accuracy. Even though a sensitivity analysis is required in order to verify if their choice is critical, here these parameters are strictly assigned following the guidelines suggested by the sub-grid model's authors [2]. In this way, the whole set of empirical constants is fixed or chosen in a predetermined way, avoiding any particular tuning aiming at matching the experimental results.

A different grid of ($1000 \times 5 \times 5$) cells was also adopted to verify the accuracy in the case of very large grid, when the sub-grid option is mandatory. The computed terminal steady flame speed is $854\,\text{m s}^{-1}$, with a difference of about 7% with respect to the experimental value. This value is substantially unchanged with respect to the value obtained with the fine grid.

With regard to the acceleration phase, Fig. 3 compares the flame speed S_f computed at different positions along the tube axis using the solid and sub-grid options, for the methane–air mixture and the fine grid ($2500 \times 10 \times 10$). Both cases show that the transition to fast propagation regime is achieved at the beginning of the tube. This result shows that the two different models do not affect the flame acceleration over the initial stages of the flame development. The transition from laminar to turbulent flame propagation regime is rapidly reached. This occurrence is due to the simplified treatment of the chemical source term, which is specifically designed to the turbulent combustion regime.

The sub-grid approach has been adopted for all the simulations presented afterward.

3.2.2. Effect of the grid size

The comparison of the calculated steady flame speeds obtained adopting several grid sizes with respect to the experimental results are reported in Fig. 4 for stoichiometric methane–air and propane–air mixtures, case (a), tube diameter $0.05\,\text{m}$, $11\,\text{m}$ long, BR $= 0.44$.

Similar trends are obtained for the methane–air and propane–air mixtures. Starting from the very coarse grids, the results firstly converge to values higher that the experimental ones.
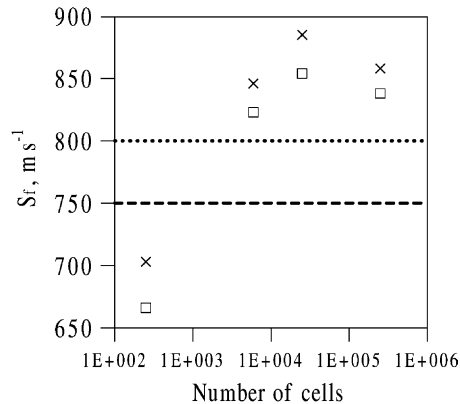
Fig. 4. Flame speeds calculated for the case (a): BR $= 0.44$, $L = 11$ m, $\phi = 1$, adopting the sub-grid option, using different grid sizes ($250 \times 1 \times 1$; $660 \times 3 \times 3$; $1000 \times 5 \times 5$; $2500 \times 10 \times 10$; ($\square$) methane (dotted line: experimental value); ($\times$) propane (dashed line: experimental value)).

However, when adopting the finer grid, a new trend is observed towards the experimental values of the terminal flame speeds, due to the direct description of the complex flow field.

In the case of the coarsest grid ($250 \times 1 \times 1$), methane–air mixture simulation gives an error of 17% while propane–air simulation gives an error of about 6%. Increasing the grid size, methane–air simulations rapidly approach better accuracy, while propane–air worsen, recovering accuracy only for the very fine grid. In any case, errors are always below the 18% and the essential features of the phenomena are always reproduced.

The effect of grid has been also evaluated for the case (b) comparing the results obtained using a very coarse grid composed by 200 cubic cells ($50 \times 2 \times 2$) and by a refined numerical grid composed by about 220,000 cubic cells ($500 \times 21 \times 21$). In this case, the calculated flame speed is 1037 m s^{-1} for the coarse grid and 994 m s^{-1} for the refined grid, both in satisfactory agreement with the experimental value of 990 m s^{-1}.

It results that the validity of the sub-grid model assumptions are better satisfied in case (b), owing to the smaller obstacle size and a more uniform pattern of the turbulent field. It is worth to say that, as far as the steady flame speed is concerned, the coarse grid coupled with the "sub-grid" modelling results to be valid to reproduce the experimental results unless transition to quasi-detonation and CJ-detonation (see next paragraphs) and very low reactivity mixtures are considered.

To evaluate the effects of grid size also in the transient acceleration phase (Fig. 5), the flame speeds computed along the tube axis for two different grid sizes are reported for methane and propane air mixtures. It clearly appears that the flame acceleration is delayed when the coarser grid is adopted: strong acceleration terminates after about 2 m in the case of the finer grid, while it prolongs up to more than 3 m in the case of the coarser grid. Comparison with experimental results is very difficult: all experimental data exhibit large scatter of single point measures, especially in the first meters of the tube, and measures collapse only when relevant to the last meters. However, computational results roughly agree with the data reported in [16,17] which indicate the acceleration phase to complete in the first 3 m of the tube.
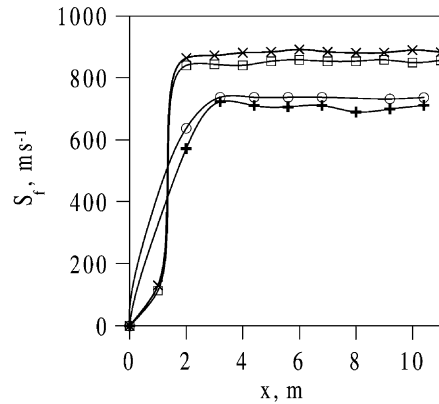
Fig. 5. Flame speed computed along the tube axis for the case (a): BR = 0.44, $L = 11$ m, $\phi = 1$, by using 250 cubic cells ((+) methane; (○) propane); and by using $1000 \times 5 \times 5$ cubic cells ((□) methane, (×) propane).

In the following sections, we adopted the choice to model all experimental tests with the coarsest grid. This choice is motivated by the intention to provide an estimate of the results when numerical prediction is obtained in a very gross way such as used in real application. Furthermore, the results do not show that much better accuracy is obtained by slightly refining the grid. Of course better results are guaranteed by adopting very fine grids; however, in this case most of the features of the flow became directly described instead that modelled, vanishing the effort for the model validation, and leading to prohibitive computational effort.

3.2.3. Effect of scale and geometry

Table 2 reports the experimental and the calculated terminal flame speeds for stoichiometric fuel mixtures with air within tubes—cases (a) and (b)—using the coarse grids defined

Table 2

Calculated ($S_{f,calc}$) and experimental ($S_{f,exp}$) flame speeds and relative error (Err) for different tube geometry and fuel–air mixtures at stoichiometric concentration

Tube geometry					Methane			Propane			Hydrogen		
BR	L (m)	D (m)	A/A^0	a/a^0	$S_{f,calc}$ (m s^{-1})	$S_{f,exp}$ (m s^{-1})	Err (%)	$S_{f,calc}$ (m s^{-1})	$S_{f,exp}$ (m s^{-1})	Err (%)	$S_{f,calc}$ (m s^{-1})	$S_{f,exp}$ (m s^{-1})	Err (%)
0.28	11	0.30	36	46	721	740	2.6	754	770	2.1	979	1900[a]	48.5
0.39	11	0.15	9	9.8	707	750	5.7	741	810	8.5	1392	1490	6.6
0.39	18	0.15	9	9.8	696	840	17.1	728	1300[b]	44.0	1268	1750[b]	27.5
0.41	7	0.30	36	33	866	1064	18.6	879	1610[b]	45.4	1462	1632[b]	10.4
0.44	11	0.05	1	1	666	800	16.7	703	750	6.3	1302	1420	8.3
0.44	18	0.05	1	1	669	700	4.4	706	800	11.7	1304	1600	18.5
0.44	18	0.30	36	36	719	745	3.5	754	1440[b]	47.6	1422	1880[a]	24.4

Coarse grids (as reported in the text) coupled with sub-grid option for all simulations.

[a] CJ-detonation regime.

[b] "Quasi-detonation" regime.

in the previous paragraph. In the case of the 18 m long tube a coarse grid composed by $814 \times 1 \times 1$ cells has been used. The ratio of orifice sections to the smallest orifice (a/a^0) and the tube section to the smallest section (A/A^0) are also reported to take into account the effect of scale.

The data show that the lower the steady flame speed attained in the single experiment the better the reproduction of the experimental values. Errors are generally below an accuracy limit of 18% with the exception of the results relevant to very fast propagation regimes, i.e. the quasi-detonation regime or the CJ regime, clearly indicating the inadequacy of the code to reproduce such propagation regimes.

The experimental results show a slight increase of the terminal flame speed when increasing the scale (A/A^0 and a/a^0) unless a transition to detonation is observed. It is also clear that the flame acceleration is strongly determined by the thermodynamic properties of the mixture. Moreover, more confidence should be addressed to the 18 m long tube. Indeed, in this case the experimental terminal flame speed is determined averaging over a longer tube length and smoother flow behaviour is observed [6].

The transition to quasi-detonation experimentally observed in the case of propane–air mixtures in the 18 m long, circular tube (BR $= 0.44$; $D = 0.15$ and 0.30 m), and in the square tube, has never been predicted by AutoReagas©. However, the code is able to predict the higher flame speed for the square tube, where the complex obstacle geometry enhances the turbulent mixing. Finally, the CJ-detonation regime has not been predicted in the case of hydrogen–air mixtures.

It is worth noting that a refinement of the grid obtained by doubling the number of computational cell along the tube axis was needed in order to model stoichiometric and off-stoichiometric hydrogen–air mixtures. Indeed, particularly in the case of mixtures with the fuel concentration close to the flammability limits, the numerical solution shows the instantaneous combustion of the whole mixture ahead of the flame front in the last meters of the tube length. Numerical instability seems to be induced by the smooth product concentration gradient computed across the flame which allows the chemical reaction to start even far from the flame front, according to Eq. (1).

3.2.4. Effect of mixture reactivity

The computed flame speeds attained for the cylindrical tube ($D = 0.3$ m, $L = 18$ m) and for the square tube using methane, propane and hydrogen–air mixtures at different equivalence ratios ϕ, are reported in Figs. 6–8. The coarse computational grids defined in the previous paragraphs have been used. Experimental results are also reported for comparison.

AutoReagas© predicts the general trend of the experimental data. The deviation from the stoichiometric condition leads to the decrease of the terminal flame speed. However, the transition to quasi-detonation or CJ-detonation has never been predicted for the propane– and hydrogen–air mixtures.

As far as the effect of the equivalence ratio is concerned, experimental evidence suggests that the flame speeds strongly depend on the mean displacement flow velocity. The latter depends on the product of the burning velocity and the density ratio across the flame. Both of these parameters decrease as the mixture composition deviates from stoichiometry, thus, leading to lower flame speeds. In AutoReagas©, the burning velocity depends on turbulence
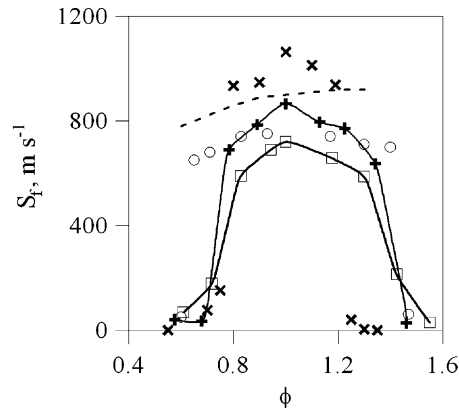
Fig. 6. Flame speed computed for the circular section tube ($D = 0.3$ m, BR $= 0.41$, $L = 18$ m; (□) calculated; (○) experimental); and for the square section tube ((+) calculated; (×) experimental). Methane–air at different equivalence ratio ϕ. Dashed line represents the isobaric speed of sound of product.

according to Eq. (2). Therefore, a larger calculated flame speed should correspond to a higher turbulence level at the flame front predicted by the code.

Table 3 collects the turbulence intensity and the turbulent burning velocity as calculated by the code, for different equivalence ratios. This data has been obtained by averaging the mean values of turbulent intensity and burning velocity over the whole cross section along the tube length once the steady flame front is established.

The effect of mixture reactivity on burning velocity is reproduced by the adopted code. However, it has to be pointed out that the numerical results have been obtained with a coarse grid and hence the predicted turbulence intensity has to be considered only for
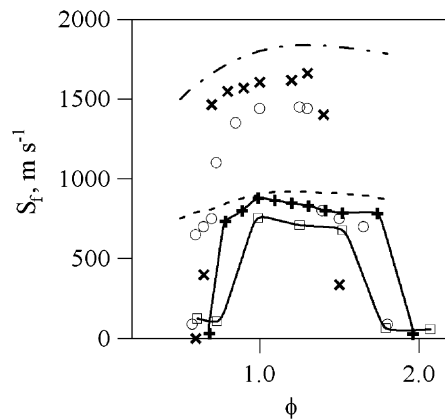

Fig. 7. Flame speed computed for the circular section tube ($D = 0.3$ m, BR $= 0.41$, $L = 18$ m; (□) calculated; (○) experimental); and for the square section tube ((+) calculated; (×) experimental). Propane–air at different equivalence ratio ϕ. Dashed line represents the isobaric speed of sound of product; dashed–dotted line represents the Chapman–Jouguet velocity.
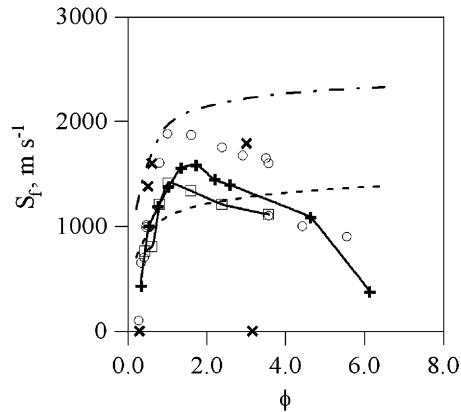
Fig. 8. Flame speed computed for the circular section tube ($D = 0.3$ m, BR $= 0.41$, $L = 18$ m; ($\Box$) calculated; ($\bigcirc$) experimental); and for the square section tube (($+$) calculated; ($\times$) experimental). Hydrogen–air at different equivalence ratio ϕ. Dashed line represents the isobaric speed of sound of product; dashed–dotted line represents the Chapman–Jouguet velocity.

comparative purposes and not as representative of the effective local turbulence generated by the obstacles.

In order to explain how the numerical model is able to reproduce the strong terminal flame speed enhancement even for small increase of the equivalence ratio, Fig. 9 reports the profiles of the fuel mass fraction, the $R_{\min}$ and turbulent kinetic energy k for the two cases at $\phi = 0.730$ and 0.753 reported in Fig. 7 (propane–air, case (a)). The reported profiles refer to three consecutive time steps ($\Delta t = 1 \times 10^{-3}$ s) relative to the transition phase from the laminar to the turbulent flame propagation. The term k affects the reaction rate by means of S_t, which is proportional to u_t through Eq. (2). $R_{\min}$ contributes directly to the reaction rate and was evaluated from the computed mixture fraction. A small increase of the reactivity of the mixture due to the increase of ϕ does not generate a great enhancement of the levels of turbulence and $R_{\lim}$. However it appears that a different interaction of the two terms is

Table 3
Mean turbulence intensity (u_t) and turbulent burning velocity (S_t) computed by AutoReagas© at the flame front

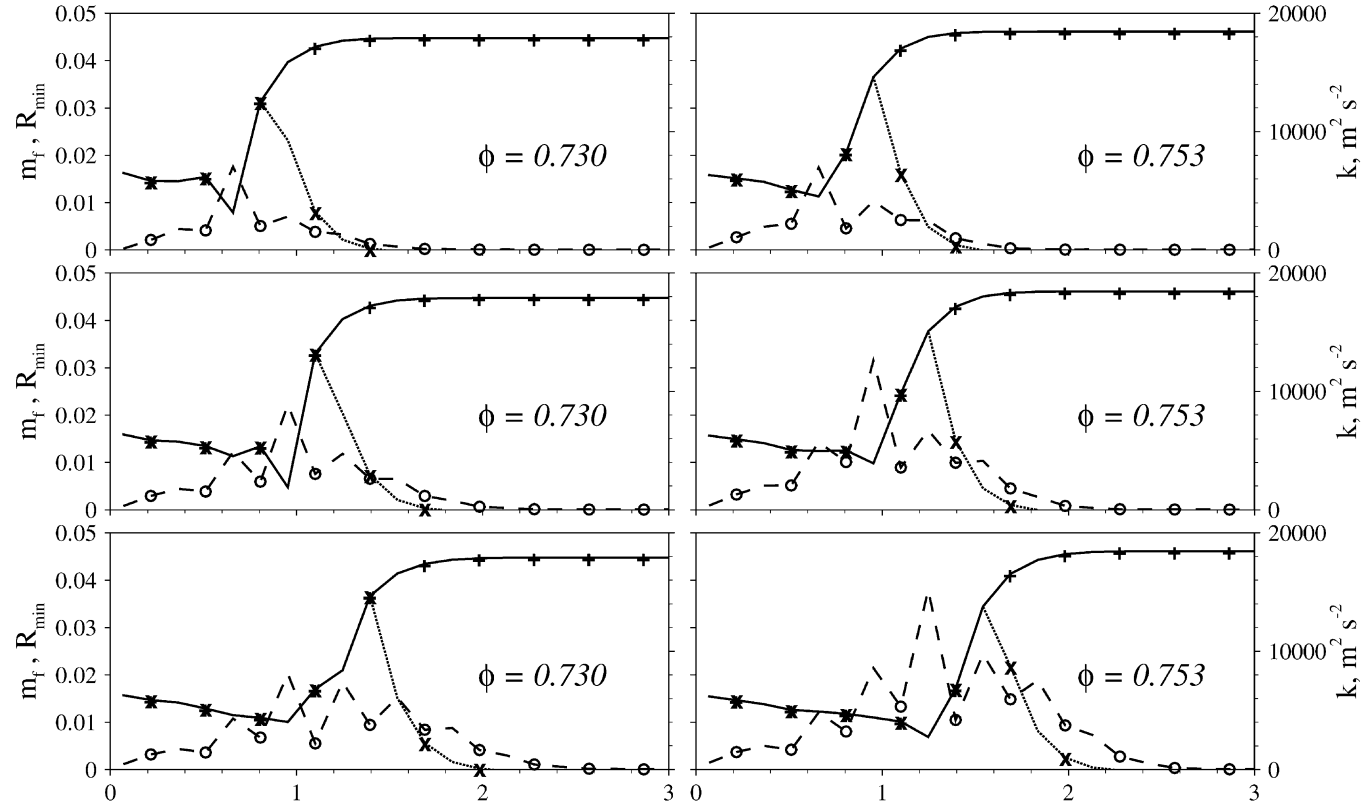| ϕ	u_t (m s^{-1})	S_t (m s^{-1})
Methane		
0.8	88.6	9.42
1.0	138	16.8
1.3	50.3	7.81
Propane		
0.8	104	8.11
1.0	141	19.0
1.5	120	11.8

$L = 11$ m, $D = 5$ cm, BR $= 0.44$.

Fig. 9. Profiles at different time steps of computed fuel mass fraction (+), R_{min} (×) and turbulent kinetic energy k (○), during the transition from laminar to turbulent flame propagation, for the square section tube with propane–air mixture at close equivalence ratios ϕ.

realised in the two cases: the maximum of R_{lim} coincides with a relative maximum of k only in the case of $\phi = 0.753$, thus, producing the higher reaction rate. It is worth to note that after the transition phase a higher intensity of k is established, although it does not appear the main effect allowing the numerical establishing of the higher flame speed propagation. Similar analyses of this interaction for other computed equivalence ratios confirm this behaviour.

4. Conclusions

In the present work, a validation study aimed at assessing the ability of the CFD code AutoReagas© to simulate the gas explosion behaviour in obstructed environments has been carried out.

The calculated terminal flame speeds attained in obstacle-filled tubes, using very coarse grids coupled with sub-grid option, show average deviations of about $80 \, \mathrm{m \, s^{-1}}$ (approximately 9%) with respect to the experimental observations as far as choking regime is considered. AutoReagas© results inadequate in handling highly reactive gases like hydrogen and is not able to reproduce the transition from the choking regime to the quasi-detonation or CJ-detonation regime, which has been experimentally observed.

The prediction of the influence of scale, geometry and mixture equivalence ratio has been proved to be in agreement with experimental trends.

Insight on the computed flame structure during the flame acceleration phase has suggested the numerical mechanism responsible for the abrupt change in the flame speed.

For the proposed configuration, the validity limit of the AutoReagas© numerical predictions have been clearly assessed. The proposed type of analysis, which include the testing of various aspects of a complex numerical simulation, such as the effect of grid size and model definition, but also the effect of the mixture reactivity, should be extended to several configurations and adopted as preliminary test by any professional operator involved with the use of any CFD code in practical application. This is expected to be very effective in enhancing both the confidence of the operators in setting the many empirical parameters that usually appears in the CFD codes and the ability to detect unphysical solutions.

References

[1] P.S. Barsanti, K.N.C. Bray, R.S. Cant, Modelling of confined turbulent explosions, in: J.R. Bowen (Ed.), Dynamics of Exothermicity: Combustion Science and Technology Book Series, Gordon and Breach, London, 1996.

[2] N.R. Popat, C.A. Catlin, B.J. Arntzen, R.P. Lindstedt, B.H. Hjertager, T. Solberg, O. Saeter, A.C. Van den Berg, J. Hazard. Mater. 45 (1996) 1–25.

[3] F.P. Lees, Loss Prevention in the Process Industries, Butterworths, London, 1996.

[4] J.H.S. Lee, R. Knystautas, C.K. Chan, in: Proceedings of the 20th International Symposium on Combustion, Pittsburgh, PA, 1984, pp. 1663–1672.

[5] I.O. Moen, J.H.S. Lee, B.H. Hjertager, K. Fuhre, R.K. Eckhoff, Combust. Flame 47 (1982) 3–52.

[6] O. Peraldi, R. Knystautas, J.H.S. Lee, in: Proceedings of the 21st International Symposium on Combustion, Pittsburgh, PA, 1986, pp. 1629–1637.

[7] A. Teodorczyk, J.H.S. Lee, R. Knystautas, in: Proceedings of the 23rd International Symposium on Combustion, Pittsburgh, PA, 1990, pp. 735–741.

 [8] S.V. Patankar, Numerical Heat Transfer and Fluid Flow, Hemisphere Publishing Corporation, Washington, DC, 1980.
 [9] B.E. Launder, D.B. Spalding, Mathematical Models of Turbulence, Academic Press, London, 1972.
[10] V. Tufano, M. Maremonti, E. Salzano, G. Russo, J. Loss Prevent Process Ind. 11 (1988) 169–175.
[11] K.N.C. Bray, Proc. Roy. Soc. London A431 (1990) 315–325.
[12] A.C. Van den Berg, H.G. The, W.P.M. Mercx, Y. Mouilleau, C.J. Hayhurst, in: Proceedings of the 8th International Symposium of Loss Prevention and Safety Promotion in the Process Industries, Vol. 1, Antwerp, Belgium, 1995, pp. 349–364.
[13] J.R. Bakke, Numerical simulation of gas explosions in two-dimensional geometries, D.Sc. Thesis, University of Bergen, Bergen, 1986.
[14] J. Chao, M. Kolbe, J.H.S. Lee, in: Proceedings of the 17th ICDERS, Heidelberg, Germany, 1999.
[15] W.E. Baker, P.A. Cox, P.S. Westine, J.J. Kulesz, R.A. Strehlow, Explosion Hazards and Evaluation, Elsevier, Amsterdam, 1983.
[16] R. Knystautas, J.H.S. Lee, O. Peraldi, C.K. Chan, Transmission of a flame from a rough to a smooth-walled tube, Dynamics of Explosions: Progress in Astronautics and Aeronautics, Vol. 106, AIAA, New York, 1986.
[17] O. Peraldi, R. Knystautas, J.H.S. Lee, in: Proceedings of the 21st International Symposium Combustion, The Combustion Institute, 1986, pp. 1629–1637.